



Modeling historical budget for β -Hexachlorocyclohexane (HCH) in the Arctic Ocean: A contrast to α -HCH



Pu-Fei Yang^{a,b}, Robie W. Macdonald^{c,d}, Hayley Hung^e, Derek C.G. Muir^f,
Roland Kallenborn^g, Anatoly N. Nikolaev^h, Wan-Li Ma^{a,b}, Li-Yan Liu^{a,b}, Yi-Fan Li^{a,b,i,*}

^a International Joint Research Center for Persistent Toxic Substances (IJRC-PTS), State Key Laboratory of Urban Water Resource and Environment, School of Environment, Harbin Institute of Technology, Harbin, 150090, China

^b International Joint Research Center for Arctic Environment and Ecosystem (IJRC-AEE), Polar Academy, Harbin Institute of Technology, Harbin, 150090, China

^c Institute of Ocean Sciences, Department of Fisheries and Oceans, Sidney, BC, V8L 4B2, Canada

^d Centre for Earth Observation Science, University of Manitoba, Winnipeg, R3T 2N2, Canada

^e Air Quality Processes Research Section, Environment and Climate Change Canada, Toronto, Ontario, Canada

^f Canada Centre for Inland Waters, Environment and Climate Change Canada, Burlington, Ontario, Canada

^g Faculty of Chemistry, Biotechnology and Food Sciences (KBM), Norwegian University of Life Sciences (NMBU), NO-1433 As, Norway

^h Institute of Natural Sciences, North-Eastern Federal University, Russia

ⁱ IJRC-PTS-NA, Toronto, Ontario, M2N 6X9, Canada

ARTICLE INFO

Article history:

Received 7 August 2022

Received in revised form

25 November 2022

Accepted 25 November 2022

Keywords:

β -Hexachlorocyclohexane

Arctic Ocean

Mass balance model

Budget

Air-water exchange

ABSTRACT

The historical annual loading to, removal from, and cumulative burden in the Arctic Ocean for β -hexachlorocyclohexane (β -HCH), an isomer comprising 5–12% of technical HCH, is investigated using a mass balance box model from 1945 to 2020. Over the 76 years, loading occurred predominantly through ocean currents and river inflow (83%) and only a small portion via atmospheric transport (16%). β -HCH started to accumulate in the Arctic Ocean in the late 1940s, reached a peak of 810 t in 1986, and decreased to 87 t in 2020, when its concentrations in the Arctic water and air were $\sim 30 \text{ ng m}^{-3}$ and $\sim 0.02 \text{ pg m}^{-3}$, respectively. Even though β -HCH and α -HCH (60–70% of technical HCH) are both the isomers of HCHs with almost identical temporal and spatial emission patterns, these two chemicals have shown different major pathways entering the Arctic. Different from α -HCH with the long-range atmospheric transport (LRAT) as its major transport pathway, β -HCH reached the Arctic mainly through long-range oceanic transport (LROT). The much higher tendency of β -HCH to partition into the water, mainly due to its much lower Henry's Law Constant than α -HCH, produced an exceptionally strong pathway divergence with β -HCH favoring slow transport in water and α -HCH favoring rapid transport in air. The concentration and burden of β -HCH in the Arctic Ocean are also predicted for the year 2050 when only 4.4–5.3 t will remain in the Arctic Ocean under the influence of climate change.

© 2022 The Authors. Published by Elsevier B.V. on behalf of Chinese Society for Environmental Sciences, Harbin Institute of Technology, Chinese Research Academy of Environmental Sciences. This is an open access article under the CC BY-NC-ND license (<http://creativecommons.org/licenses/by-nc-nd/4.0/>).

1. Introduction

Hexachlorocyclohexanes (HCHs) are cheaply-produced organochlorine pesticides (OCPs), which are classified as persistent organic pollutants (POPs). The HCHs, which entered into

widespread use during the 1940s, have been produced as technical HCHs containing four stable isomers (α : 60–70%, β : 5–12%, γ : 10–12%, δ : 6–10%) [1], and Lindane®, which consists of almost pure γ -HCH (>99%). The production and use of technical HCH increased with time following its introduction in the 1940s in Europe and North America and was curtailed in the 1990s. The total global usage of technical HCH has been estimated at 10 Mt between 1948 and 1997 [2–4], the highest among all chlorinated pesticides used worldwide.

After application in source regions, HCH compounds can be transported to the Arctic through atmospheric long-range

* Corresponding author. International Joint Research Center for Persistent Toxic Substances (IJRC-PTS), State Key Laboratory of Urban Water Resource and Environment, School of Environment, Harbin Institute of Technology, Harbin, 150090, China.

E-mail address: dr_li_yifan@163.com (Y.-F. Li).

transport (LRT) and water pathways (river discharges and ocean currents). The first report of α - and γ -HCHs in the Arctic air was dated in 1979 [5], while β -HCH in the Arctic air was reported much later in 1988 [6].

Clarifying sources and pathways of industrial and agricultural POPs to the Arctic have been major objectives of Arctic research and contaminant assessments [7,8]. In this regard, HCHs compounds, α -HCH, and β -HCH in particular, have played an exceptional role in understanding the connections between sources and sinks because environmental loadings have led to concentrations that are relatively easy to measure. Thus, budgets and distributions of HCHs have become far better understood than those for other POPs [4,7].

Atmospheric LRT has traditionally been considered the primary pathway by which semi-volatile contaminants (SVOCs) enter the Arctic, as evidenced by extensive research on α -HCH [4,7,9–12]. The first direct evidence that air was a predominant medium of transport into the Arctic was the strong correlation between concentrations of α -HCH in the Arctic air and technical HCH global usage [10] and global emissions of α -HCH [11], which clearly demonstrated rapid atmospheric dispersion of α -HCH from source regions into the Arctic.

To understand how α -HCH loaded into the Arctic Ocean and how long it might take for the Arctic Ocean to respond to diminishing atmospheric loadings due to global control measures, Li and co-workers [10] developed an Arctic Mass Balance Box Model Version 1 (AMBBM 1.0), which has been successfully applied to simulate the historical budgets in the Arctic Ocean for α -HCH. In this model, global emission history [13] together with flux estimates into and out of the Arctic Ocean, produced annual mass balances from 1945 to 2000. The model results compared well with published monitoring data from the samples collected during the 1980s and 1990s [7,14]. It turned out that α -HCH started to accumulate in the Arctic Ocean in the late 1940s, reached the highest estimated value of 6670 t in 1982, and decreased to 1550 t in 2000. The total estimated loading for the entire period between 1945 and 2000 was 27700 t, with gas absorption as the main input pathway (50%) followed by ocean currents (34%) [10]. These results confirmed the commonly held assumption that atmospheric LRT was the primary pathway by which semi-volatile contaminants enter the Arctic, but it also showed that water-borne pathways could not be neglected, at least for some POPs.

The success in modeling α -HCH in the Arctic Ocean supported the notion that atmospheric transport was, in general, the predominant mode of entry into the Arctic Ocean for all POPs, as expressed in the first Canadian Arctic Contaminants Assessment Report [15], “contaminants such as persistent organic contaminants (POPs), heavy metals and radionuclides enter the Arctic through long-range transport on air and water currents, with the atmosphere being the *primary pathway*”. This view was challenged by Li and co-workers [16] who showed that the primary pathway for β -HCH to enter the Arctic Ocean had to be ocean currents. In that study, the authors proposed that much of the β -HCH emitted from Asia was deposited into the strongly stratified North Pacific Ocean and the Bering Sea by rainfall and gas–water exchange. This β -HCH subsequently enters the western Arctic Ocean following ocean currents from the Pacific Ocean through the Bering Strait. One could anticipate a parallel set of circumstances to affect a pathway separation between α -HCH and β -HCH in the North Atlantic Ocean, which feeds the Eastern Arctic Ocean, and given that the volumetric flows are much larger through the Fram Strait than the Bering Strait, oceanic transport could be even more important.

Following the conjecture that β -HCH was transported to the Arctic Ocean mostly by water, not air, subsequent research has confirmed the decoupling of α -HCH and β -HCH's pathways to the Arctic, and the effects may be seen in both water and biota [4]. The

consequence of separation between the two isomers is reflected in spatial variations in water concentrations; for example, early in the history of HCH emissions, the preferential loading of β -HCH into the Bering Sea led to β -HCH enrichments in that region [17] which then subsequently loaded into the Chukchi Sea, just as the higher atmospheric deposition of α -HCH into the Canada Basin surface waters initially led to α -HCH enrichments that subsequently loaded into the Canadian Archipelago and, eventually, in the Labrador Current [18]. In the interior surface waters of the Arctic Ocean, the concentrations of α -HCH reached a value of 7 ng L⁻¹, compared to 0.2 ng L⁻¹ or lower for β -HCH. In contrast, the Bering and Chukchi Seas achieved high surface water concentrations for β -HCH (~1.2 ng L⁻¹), more comparable to α -HCH (~3.2 ng L⁻¹), during the 1990s. Perhaps more importantly, regarding potential biological impact, such aquatic distributions were also reflected in resident biota [19–23]. These elegant examples of how food webs reflect large-scale contaminant transport dictated by environmental processes underscore the importance of understanding and modeling the environmental fate of the β isomer, which may provide valuable insight into its distribution in the Arctic Ocean and its potential effects. This divergence in transport pathways between α -HCH and β -HCH presents the most extreme case that we know of favoring the transport and accumulation in water, given that aquatic food webs tend to be at greatest risk from these chemicals.

Their different physical-chemical properties cause the separation of α -HCH and β -HCH in LRT. β -HCH has stronger lipophilicity, water solubility, and longer half-life than α -HCH. Modeling can estimate POPs' properties and their environmental behavior. Although the budget and fate of α -HCH in the Arctic Ocean were successfully modeled by the AMBBM 1.0, the modeling focusing on the β -HCH was scarce because it is a considered less important isomer in the technical mixture and accumulates relatively little in the environment. Wöhrnschimmel et al. [24] studied the fate of both α -HCH and β -HCH before and after being phased-out and compared their difference using the BETR Global 2.0 model. In their study, the relationship between HCHs' fate and their physical-chemical properties was further elucidated by comparing modeled and observed levels and trends in air and water; the influence of climate change was also included. However, the reported study did not discuss the budget of either α -HCH or β -HCH.

Encouraged by the successful modeling of the budget and fate of α -HCH in the Arctic Ocean, in this work, we study the historical annual loading to, removal from, and cumulative burden in the Arctic Ocean in 1945–2020 for β -HCH using a modified Arctic Mass Balance Box Model (AMBBM 2.0) similar to that applied to α -HCH earlier [10]. We examine the period between 1945, the year this compound was introduced into widespread use, and 2020. The model takes into account the known chemical properties of β -HCH (Table S1), the emission history, and various mechanisms that control fluxes into and out of the Arctic Ocean (seawater exchange via ocean currents, air–sea exchange, river inflow, sea ice cover, degradation and loss to deep water). The model output includes estimates of compartments' concentrations, loading to and removal from the Arctic Ocean, and the budget of β -HCH in the upper ocean in any given year from 1945 to 2020. Thus, the environmental behavior of β -HCH in the Arctic and the source region are investigated, and the projections of the budget for β -HCH for 2020–2050 are also presented in the paper.

2. Methods

2.1. AMBBM 2.0

The Arctic mass balance box model (AMBBM 1.0) was developed in 2004 [10] and was used to calculate the budget of the α -HCH in

the Arctic Ocean. A variety of loading or removal pathways of α -HCH was discussed in the model. Here, AMBBM version 2.0 is developed based on AMBBM 1.0 and has the following modifications (Table 1).

2.2. Spatial and temporal design

AMBBM 2.0 takes the Northern Hemisphere as the model domain, divided into two portions: the Source Zone and the receiving Arctic Zone, separated by the latitude of 66.5° N (Arctic circle). The total area of the Arctic Zone is $2.13 \times 10^{13} \text{ m}^2$, with the Arctic Ocean as the largest compartment ($1.34 \times 10^{13} \text{ m}^2$) and the rest being land ($7.90 \times 10^{12} \text{ m}^2$). The area of the Source Zone ($2.4 \times 10^{13} \text{ m}^2$) is divided by land ($9.6 \times 10^{13} \text{ m}^2$) and ocean ($1.44 \times 10^{14} \text{ m}^2$). Area data was calculated through the GDAM dataset (<https://gadm.org/>) on the ArcGIS platform. The spatial coverage is shown in Fig. 1a. SVOCs are emitted into the Source Zone, where they redistribute in air, ocean, and soil, some of which are transported to the Arctic through LRAT and LROT, where they can exchange between compartments. All relevant environmental processes among the atmosphere (“air” for short), surface ocean including seawater and sea ice (“ocean” for short), and land surface including surface soil and snowpack (“land” for short) are estimated in the model.

AMBBM 2.0 is a level IV fugacity model with a steady P/G partitioning component for POPs in the atmosphere, calculating the long-term environmental behavior of these chemicals in the Arctic. For β -HCHs, global usage started in 1945 in general. Here, 1945–2020 is chosen as the target time scale. In the model, average results are given for every six months, named the cold and the warm seasons. For simplicity, we assume the cold season starts on November 1 in the previous year and ends on April 30 of the current year, whereas the warm season is from May 1 to October 31, as shown in Fig. 1b. The emission rate in the Source Zone and environmental properties in the Arctic Zone are set differently in different season. Precipitation in the Arctic occurs in two forms. The precipitation happens mainly in the form of rain in the warm season and snow in the cold season. The surface coverages of snowpack on the land and sea ice on the ocean also change seasonally. In the cold season, all soil is frozen and covered with snowpack, and 50% of the ocean is covered with sea ice, whereas in the warm season, 60% of surface soil is bare, and only 35% of the Arctic surface is covered with sea ice [24,26]. Snow and ice's melting and freezing are treated as ongoing processes, and assumed to occur instantly in the model. The fourth-order Runge-Kutta method solves ordinary differential equations describing the above mentioned environmental processes. The time steps are prescribed in the model as one day.

For the sake of simplicity, no seasonal temperature change is assumed in the source area, $T_{\text{Air_Source}} = 15 \text{ }^\circ\text{C}$ and $T_{\text{Ocean_Source}} = 15 \text{ }^\circ\text{C}$. However, temperatures in different season and media are different in the Arctic zone. According to the “NCEP/

NCAR Reanalysis I” database, the air temperature in the warm season, $T_{\text{Air_Arctic_Warm}} = 0 \text{ }^\circ\text{C}$, whereas in the cold season, $T_{\text{Air_Arctic_Cold}} = -25 \text{ }^\circ\text{C}$. The seasonal change of the Arctic Ocean is gentler, $T_{\text{Ocean_Arctic_Cold}}$ is set to $-1.8 \text{ }^\circ\text{C}$, the freezing point of brine, whereas $T_{\text{Ocean_Arctic_Warm}}$ is set to $5 \text{ }^\circ\text{C}$ [27].

2.3. Emission

The annual emission data of β -HCH is derived from Li et al. [28]. In the present study, we assume that all technical HCH was used in the warm season in farmland by spraying droplets into surface soil or mixing into deeper soil. Thus, we assume that 95% of HCHs fell on the soil and the rest emitted into the air during their applications [24].

2.4. Particle/gas partition

The steady-state equation (Li-Ma-Yang Model) was developed explicitly to study the P/G partitioning behavior of SVOCs [25]:

$$\log K_{\text{PS}} = \log K_{\text{PE}} + \log \alpha \quad (1)$$

In the above equation, the *equilibrium term*, $\log K_{\text{PE}}$, is given by the Harner-Bidleman equation [29] as:

$$\log K_{\text{PE}} = \log K_{\text{OA}} + \log f_{\text{OM}} - 11.91 \quad (2)$$

and $\log \alpha$, the *non-equilibrium term*, is given as:

$$\log \alpha = -\log(1 + 4.18 \times 10^{-11} f_{\text{OM}} K_{\text{OA}}) \quad (3)$$

where K_{OA} is the octanol-air partition coefficient, and f_{OM} is the mass fraction of organic matter contained in aerosol particles.

The above equations lead to two thresholds of $\log K_{\text{OA}}$, $\log K_{\text{OA}1} = 11.38$ and $\log K_{\text{OA}2} = 12.50$ [30]. As shown in Fig. S1, the two thresholds partition the range of $\log K_{\text{OA}}$ into *equilibrium* (EQ), *nonequilibrium* (NE), and *maximum partition* (MP) domains, in which the values of $\log K_{\text{PS}}$ reach a maximum constant value of $\log K_{\text{PSM}} = -1.53$, independent of the values of $\log K_{\text{OA}}$ and thus the temperature.

2.5. Intermedia processes

In the AMBBM 2.0, the Arctic Zone consists of five compartments: gas, aerosol particles, seawater, sea ice, soil, and snowpack, whereas the Source Zone has three: air, soil, and water (Fig. 1a). Details of the equations used in the model to describe transport and transfer processes in the media of the two zones along with the parameters are shown in Text S1, with parameters given in Tables S1–S5, SI.

Table 1
Comparison between AMBBM 1.0 and AMBBM 2.0

| Items | AMBBM 1.0 | AMBBM 2.0 |
|---------------------------------|--------------------------------------------------------------------------------------------------------------------------------------|---------------------------------------------------------------|
| Phases considered | Air, seawater, deep water | Air, seawater, deep water, snowpack, sea ice, and soil phases |
| Processes | Gas-phase dry and wet depositions, particle-phase dry and wet depositions, volatilization, degradation, etc. | Add snowfall, melt & refreeze processes of snow and ice, etc. |
| Input data | Concentrations in the Arctic air, the seawater in the Bering Strait and the North-Atlantic Ocean, and the rivers to the Arctic Ocean | Monitoring data is no longer needed as the input data |
| Times step | One year | One day, but output data for every half year (six months) |
| Particle/gas (P/G) partitioning | Based on equilibrium theory (Harner-Bidleman Equation) | Based on the steady-state theory (Li-Ma-Yang Equation) [25] |

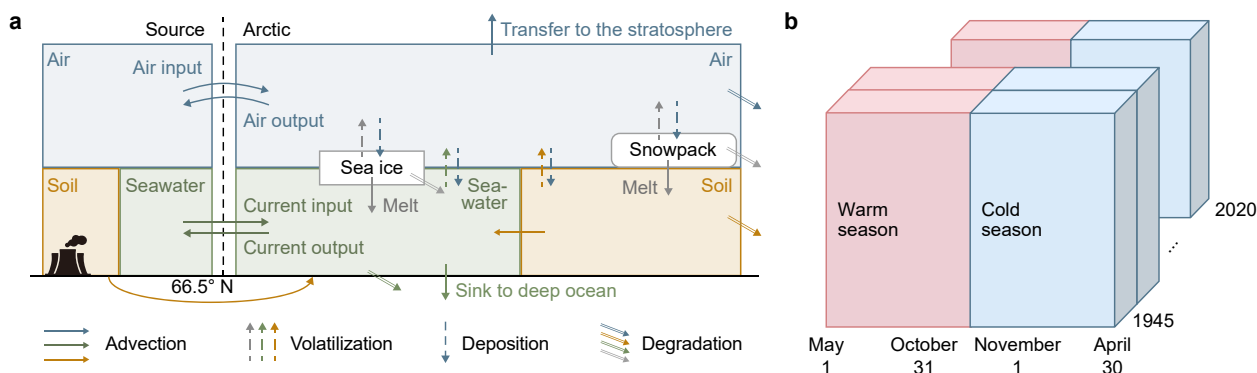


Fig. 1. a, Spatial design of AMBBM 2.0. b, Temporal design of AMBBM 2.0.

2.6. Sensitivity analysis

The sensitivity analysis of the AMBBM 2.0 is performed based on Monte Carlo analysis. As this work aims to study chemicals' budget in the Arctic Ocean influenced by their different physical-chemical properties, we choose air–water partition coefficient (K_{AW}), octanol–air partition coefficient (K_{OA}), half-lives in the air (HL_{Air}), water (HL_{Water}), and soil (HL_{Soil}) as the input properties to estimate the sensitivity of α - and β -HCH's environmental behaviors to these properties in the Arctic Ocean. A lognormal distribution is assumed for all input parameters. The dispersion factors of these properties are given in Table S6. The Monte Carlo analysis takes 3000 runs, and Spearman's rank correlation coefficient was used to calculate contributions to variance. The analysis results are given in Fig. S4.

2.7. Model evaluation

To compare the difference between the modeling result and the sampling result, the root mean square error of log-transformed concentrations ($RMSE_{log}$) [31] was calculated using the following equation (4):

$$RMSE_{log} = 10 \sqrt{\frac{1}{n} \sum_{i=1}^n [\log(C_{est.}) - \log(C_{obs.})]^2} \quad (4)$$

where $RMSE_{log}$ is the root mean square error of log-transformed, $C_{est.}$ is the estimated concentration, $C_{obs.}$ is the observed concentration, and n is the number of samples.

3. Model evaluation using α -HCH

In the previous paper, the annual budget and burden of α -HCH in the Arctic Ocean were successfully simulated by the AMBBM 1.0 [10]. To evaluate AMBBM 2.0, this model is applied to predict the annual budget and burden of α -HCH, and the results are compared with those predicted by AMBBM 1.0.

3.1. Air concentration (C_A) and gas–ocean exchange

The AMBBM 1.0 and 2.0 calculated the air concentrations (C_A) for α -HCH in the Arctic in completely different ways. C_A in the AMBBM 1.0 was calculated directly from a strong correlation between air concentrations of α -HCH in the Arctic and its global emissions. However, this correlation is not applied to calculate C_A in AMBBM 2.0, which is modeled based on the fugacity and advection methods, as mentioned in section 2.1. The concentrations predicted by both AMBBM 1.0 and 2.0 and the monitoring data [32] (<https://>

ebas.nilu.no/) in the Arctic air at Alert, Nunavut are shown in Fig. 2a, indicating the agreement between the results from these two models ($RMSE_{log}$ is 4.06 for AMBBM 1.0 and 4.05 for AMBBM 2.0). Besides, AMBBM 2.0 can provide the seasonal variation of α -HCH in the Arctic air. However, the AMBBM 2.0 smooths the two sharp decreases of α -HCH in the Arctic air, responding to the sharp decrease of its global emissions that happened at the beginning of the 1980s and in the 1990s.

The results of C_W predicted by AMBBM 1.0 and 2.0 are considered in an agreement but with a distinct difference in the early loading years from 1945 to 1950 (Fig. 2b), when the values of C_W predicted by AMBBM 1.0 are higher than those by AMBBM 2.0. This could be mainly caused by the difference in inflows of this compound in ocean/river currents described in the previous subsection. From 1960, the concentration of α -HCH predicted by the AMBBM 2.0 became larger than that predicted by the AMBBM 1.0. This is mainly caused by the stronger gas–ocean exchange process used in the former than in the latter. It turns out that AMBBM 2.0 is superior to AMBBM 1.0 in predicting the level of α -HCH in the Arctic Ocean ($RMSE_{log}$: 2.92 for AMBBM 1.0 and 2.19 for AMBBM 2.0).

The annual net flux between air and water is depicted in Fig. 2c. In years before 1990, although the calculated air concentrations from AMBBM 1.0 were higher (Fig. 2a), AMBBM 2.0 estimated stronger ocean absorption flux. Interestingly, the direction of gas–ocean exchange predicted by AMBBM 2.0 shows a change from “air to ocean water” to “ocean water to air” in the summer of 1993, which is supported by the observation reported by Jantunen and Bidleman [34], whereas the AMBBM 1.0 predicted that α -HCH reach equilibrium in the air and ocean of the North America Arctic in the same year.

3.2. Ocean current and rivers inflow

Annual inputs of α -HCH through the ocean current and river inflows predicted by both AMBBM 1.0 and 2.0 from 1945 to 2000 are presented in Fig. 3, showing that results from both the models match well although they calculated these inflows in very different ways (Table 1). The largest difference occurred in the early loading years from 1945 to 1955, when the rivers and ocean current inflows of α -HCH predicted by AMBBM 1.0 were higher than those by AMBBM 2.0. The AMBBM 1.0 estimated the input inflow of α -HCH due to the ocean currents from 1945 to 1980 simply using interpolation based on much limited monitoring data [10], while the AMBBM 2.0 treats emissions, transport, and transfer of α -HCH in multi-compartments (air, ocean, and soil) of in the Source Zone in a dynamic way, and then this chemical enters the Arctic Zone through atmospheric and ocean/river pathways. In AMBBM 2.0, it takes a few years for α -HCH to enter the ocean in the Source Zone and accumulate enough concentration in the water, and then α -

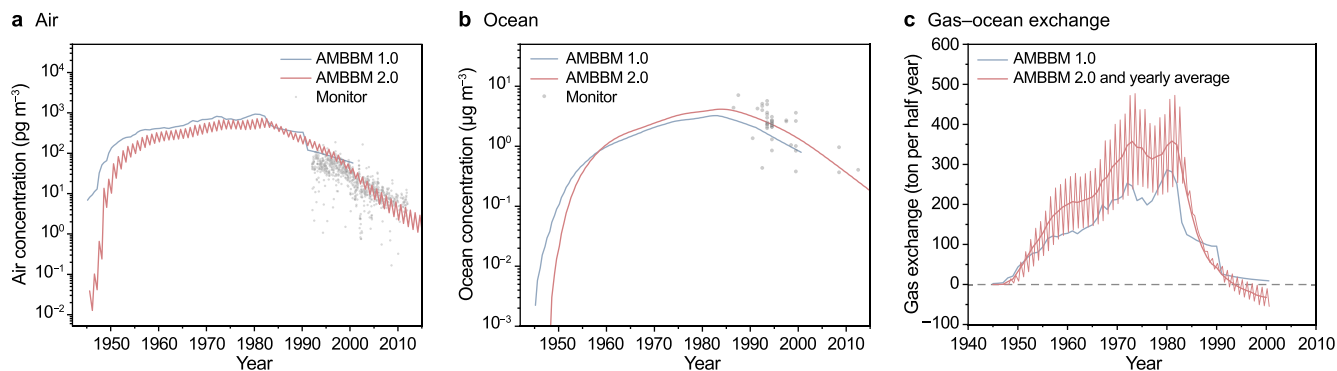


Fig. 2. a, Annual concentrations of α -HCH in the Arctic air predicted by both models (Blue line: results provided by AMBBM 1.0; pink line: results provided by AMBBM 2.0; grey dots: monitoring data [32] (<https://ebas.nilu.no/>)). b, Annual water concentrations of α -HCH in the Arctic Ocean predicted by AMBBM 1.0 and 2.0 with the monitoring data. (Sources of the monitoring data from Li et al. [10] and Wang et al. [33]). c, Annual gas-ocean exchange of α -HCH in the Arctic from 1945 to 2000 predicted by both models.

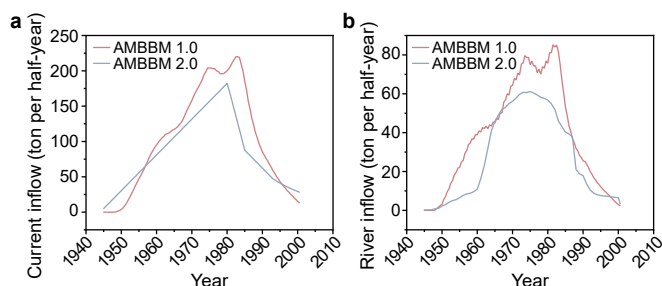


Fig. 3. Annual inputs of α -HCH in the Arctic Ocean through ocean currents (a) and river inflows (b) from 1945 to 2000 predicted by AMBBM 1.0 and 2.0.

HCH can travel to the Arctic Ocean effectively. Thus, there is a time lag for α -HCH to reach the Arctic Ocean through ocean currents compared to its atmospheric pathway simulated using the AMBBM 2.0, but not in the AMBBM 1.0. This does not significantly affect the budget of this chemical in the Arctic Ocean in the time frame of 56 years from 1945 to 2000.

3.3. Budget

The annual budgets of α -HCH produced from 1945 to 2000 by both the AMBBM 1.0 and 2.0 are depicted in Fig. 4. Both models predicted the LRAT as the major pathway for α -HCH to enter the Arctic: 51% from air predicted by AMBBM 1.0 and 59% by AMBBM 2.0, and both reckon that the ocean degradation is the most important removal pathway. AMBBM 2.0 predicts higher total loadings and removal, higher gas exchange, gas wet deposition, and loss to deep water, but lower for other processes than those predicted by AMBBM 1.0.

3.4. Burden

The annual burdens of α -HCH in the Arctic Ocean from 1945 to 2000 predicted by AMBBM 1.0 and 2.0 are shown in Fig. 5. The accumulated burden calculated by AMBBM 2.0 is almost two times larger than that by AMBBM 1.0, which is mainly due to the reasons discussed in Section 3.2, which are (1) stronger air-ocean exchange rate in AMBBM 2.0 than AMBBM 1.0 (Fig. 2c), (2) larger inflows of α -HCH through water currents in AMBBM 2.0 than AMBBM 1.0 (Fig. 3), and (3) AMBBM 2.0 defines larger Arctic Ocean than AMBBM 1.0. In the early years, the difference between these models is small. In 1960, the burden in the AMBBM 1.0 and 2.0 were 1800 t

and 3000 t. But as time progresses, the difference becomes larger. In AMBBM 1.0, the burden of α -HCH peaked in 1981 at 5200 t, but in 1984 at 11000 t predicted by AMBBM 2.0. This promoted the reversal of the direction of the gas-water exchange between air and ocean [34], which was not simulated by AMBBM 1.0. In 2000, the burden of α -HCH in the Arctic Ocean was 1600 t from the AMBBM 1.0 and 3500 t from the AMBBM 2.0.

4. Result

4.1. Concentrations of β -HCH in the Arctic

Air concentrations. Fig. 6a presents the air concentrations of β -HCH in the Arctic from 1975 to 2015. Wöhrnschimmel and co-workers [24] also evaluate β -HCH's air concentration in the Arctic using BETR-Global 2.0, and the annual highest and lowest values are indicated by two blue lines in the figure. It is interesting to note that the results from our study lie well within this range. The figure also shows that the simulated data fit well the trend of monitoring data measured in Alert, Canada, with 96.3% of measured data falling into the $\pm\log_1$ range of the model results with the $RMSE_{\log}$ value as 5.32.

Water concentrations. Fig. 6b depicts the water concentrations of β -HCH in the Arctic Ocean, showing a good agreement between the modeled data and the monitoring data, with almost all measured data within the $\pm\log_1$ range of the modeled results. β -HCH's concentration in the Arctic Ocean seems slightly over-estimated (see Fig. 6b).

Surface soil concentrations. Both the modeled and measured concentrations of β -HCH in surface soil are presented in Fig. 6c, showing that all the measured data fall in the $\pm\log_1$ area.

Concentrations in other matrices. Besides the results for the concentration of β -HCH in air, water, and surface soil, those in other matrices, such as sea ice and snowpack, are also simulated, with the results given in Fig. S2. Monitoring data of β -HCH in these two phases have not been reported yet. Hermanson et al. [35] measured the concentration of OCPs in surface snow on glacier sites in Svalbard during the cold season of 2014. The concentration of β -HCH has not been detected. Interestingly, the simulated β -HCH concentration in snowpack in the same year was $\sim 6.6 \times 10^{-4} \text{ ng L}^{-1}$, which was lower than the LOQ ($5.5 \times 10^{-3} \text{ ng L}^{-1}$) reported by Hermanson et al. [35].

4.2. Budget of β -HCH

4.2.1. Burden of β -HCH in the Arctic Ocean

As shown in Fig. 7a, the historical β -HCH's burden from 1945 to

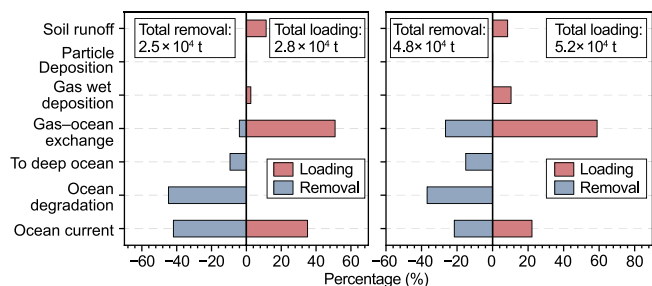


Fig. 4. The annual budgets of α -HCH in the Arctic Ocean are predicted by AMBBM 1.0 (left) and AMBBM 2.0 (right).

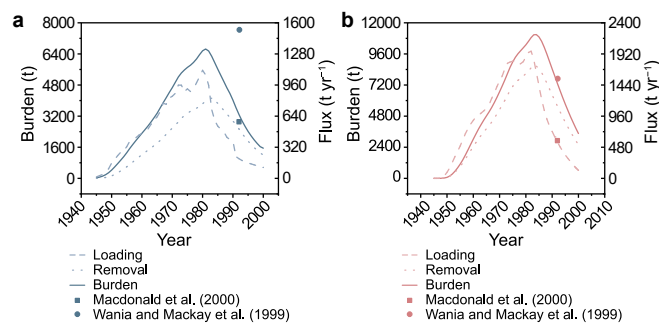


Fig. 5. Loading to, removal from, and burden of α -HCH in the Arctic waters: **a**, AMBBM 1.0; **b**, AMBBM 2.0. The square indicates the estimated burden of 2910 t in the early 1990s by Macdonald et al. [7] and the round indicates the estimated burden of 7680 t in the early 1990s by Wania and Mackay [14].

2020 in the Arctic compartments, indicating that the Seawater is the largest storage of β -HCH in the Arctic Zone, containing over 90% of β -HCH in the Arctic in most years. The dominant amount of β -HCH in the Arctic Ocean is not unexpected due to its low K_{AW} value and the huge volume and fugacity capacity of ocean water. From 1960 to 2020, the amount of β -HCH in the Arctic air was very small (<1%), whereas in the first five years, the proportion of β -HCH in the Arctic air was much higher, reaching as high as >10% in the first year. Similar to α -HCH, β -HCH can quickly arrive in the Arctic through LRAT [16], although in a very small amount, while there was a delay for β -HCH to reach the Arctic Ocean through the ocean currents, which led to a relatively high proportion of mass in the Arctic air in the first several years. Even with a relatively low

amount, the mass of β -HCH in the Arctic air is the most active and dynamic part of all the atmospheric transport and transfer processes within the Arctic environment [38,39].

It is through deposition and gas exchange that β -HCH can enter the soil and snowpack. The burden of β -HCH in soil, the second largest storage compartment of β -HCH, keeps rising in the long term because of its longer half-life in soil. Sea ice and snowpack hinder the exchange of the chemical between air and two other surface media, ocean water and soil, respectively [38–40]. Since sea ice is much thicker than snowpack and can accumulate across the year, thus, the burden of the sea ice is much larger than that in the snowpack.

Fig. 7b shows the burdens, total loadings, and total removals from 1945 to 2020. In these years, around 2700 t β -HCH enter the Arctic Ocean through different pathways, which is 1.2% of the historical global emission [16]. Two periods from 1945 to 2020 can be identified for the study according to the variation of the burdens of β -HCH in the Arctic Ocean. One is called the accumulation period (AP) from 1945 to 1986 with an increasing trend of the burden, or when the loading is larger than the removal, and the decay period (DP) from 1987 to 2020 with a decreasing trend of the burden, or when the removal exceeds the loading.

In the AP, the average annual loading in the AP is 50 t yr^{-1} , whereas the average annual removal is 30 t yr^{-1} , with the annual net average burden increased by approximately 20 t yr^{-1} . In 1986, the burden of β -HCH in the Arctic reached its peak at 810 t, five years later than the peak of α -HCH according to the prediction by AMBBM 1.0 [10]. In the DP, the yearly average removal rate and loading rates are 37 and 16 t yr^{-1} , respectively, leading to an annual net decrease rate of burden as 21 t yr^{-1} . In this period, the Arctic Ocean became an important secondary emission source that continually released β -HCH. The β -HCH burden in the Arctic Ocean decreased to 87 t in 2020.

4.2.2. Temporal variation of β -HCH budget in the Arctic Ocean

Loading and removal percentages in the 76 years and the two periods AP and DP are shown in Fig. 8a–c, showing a similar pattern for the removal and a different pattern for the loading.

The most important loading pathway in the whole period is undoubtedly ocean current inflow (71%). The contribution of gas–water exchange and soil runoff are similar (11% and 12%). Thanks to the very low precipitation, β -HCH's relatively low K_{OA} (Fig. S1), and small TSP in the Arctic atmosphere [41,42], the contribution of particle deposition and rain/snow scavenging is very limited. On the removal side, the degradation in the ocean and outflow through the ocean currents are both the most important pathways for the removal of β -HCH (37% and 35% for each). Because

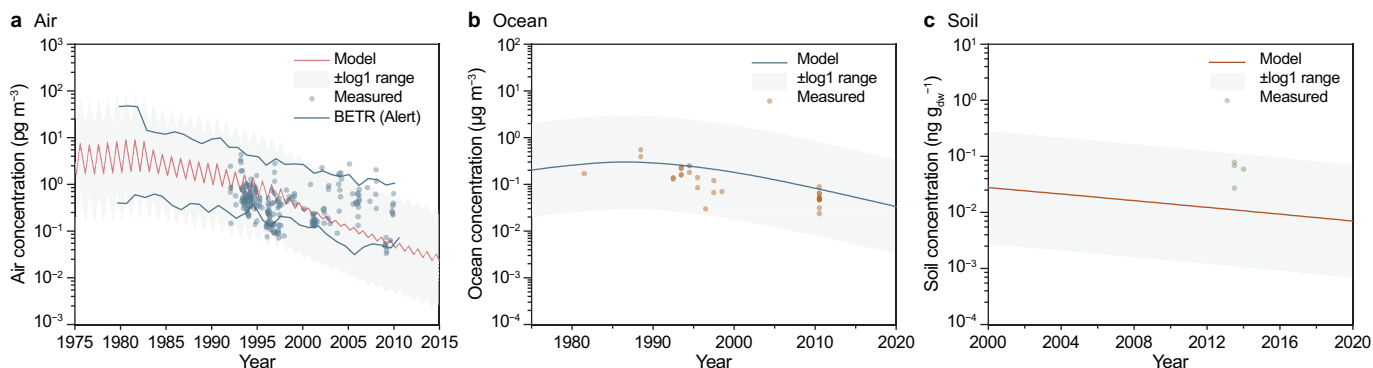


Fig. 6. **a**, Air concentration of β -HCH [32] (Monitoring data: <https://ebas.nilu.no/>), **b**, Ocean β -HCH concentration of β -HCH (Sources of the monitoring data: Li et al. [16] and Cai et al. [36]), **c**, Soil concentration of β -HCH (Sources of the monitoring data: Casal et al. [37]).

of the ocean circulation in the Arctic, a considerable amount of β -HCH is removed by entering the deep ocean (25%) [7]. However, gas–water exchange is not an important removal process for β -HCH (2%).

In the AP, the contribution to the loadings due to the gas–ocean exchange and soil runoff were more important (both reaching 13%), because in early years, air and soil contained more burden of β -HCH in the Source Zone, whereas the contribution of ocean current was building up. In DP, however, as a proportion of β -HCH in air and soil in the Source Zone reduced, and so did the deposition and runoff to the Ocean, respectively, the contribution of β -HCH in the ocean currents in the Source Zone to its loading to the Arctic Ocean increased from 68% in the AP to the 83% in the DP.

The model also estimated the budget in the Arctic air and soil, as shown in Fig. 8d and e. Compared with the Arctic Ocean, the total loading and removal of β -HCH in air and soil are much smaller. This shows that air and land contribute less to β -HCH's accumulation and removal in the Arctic. Almost all β -HCH (96%) was brought into, and more than half (65%) was brought out of the Arctic air by atmospheric circulation. Part of the rest leaves the Arctic Ocean through gas–ocean exchange (18%). The main loading and removal pathways of the land are gas–soil exchange (84%) and degradation (87%), respectively.

5. Discussion

5.1. Historical budget in the Arctic Ocean: a contrast to α -HCH

Besides β -HCH, the result of α -HCH was also estimated by AMBBM 2.0. In addition, to be used for model evaluation, it is also used as a comparison with β -HCH.

5.1.1. Emission

As two stable isomers contained in technical HCH, β -HCH and α -HCH have identical temporal and spatial trends of the primary emissions with a much larger emission amount for α -HCH than β -HCH. However, the temporal and spatial trends of volatilization from surface soil are different [28]. β -HCH is more persistent (has a longer half-life time) than α -HCH in the environment.

5.1.2. Loading to the Arctic Ocean

It has been widely accepted that α -HCH and β -HCH reached the Arctic Ocean differently. α -HCH is mainly transported through LRAT, while β -HCH mainly through LROT [16,43]. By using the model, we can quantitatively compare this difference. From 1945 to 2020, a total of 5.2×10^4 t of α -HCH entered the Arctic Ocean while the total amount of β -HCH is 2.7×10^3 t, which is $\sim 1/20$ of the α -HCH entered the Arctic Ocean. Considering β -HCH is $\sim 1/10$ of the α -

HCH in the technical HCH, β -HCH has less LRT capability than α -HCH. 69% of the total α -HCH is brought into the Arctic Ocean from the atmosphere through wet and dry deposition processes of both gas– and particle–phases, while this proportion for β -HCH is only 16%. The main loading of β -HCH via ocean currents accounts for 71% of total loading to the Arctic, while this value for α -HCH is only 22%. Loading through both LRAT and LROT were the main loading processes for both α -HCH and β -HCH, consisting of 92% and 88% of α -HCH and β -HCH's total loading, respectively. The detailed contrast is shown in Table 2.

5.1.3. Re-emission

The Arctic is a cold region, thus, chemicals in the Arctic can stay for a long time. Many POPs, including α -HCH and β -HCH, have accumulated in the Arctic, especially in the Arctic Ocean, originating from their wide use and continuous emissions worldwide. These POPs in the Arctic form secondary sources. As the primary emissions were weakened, the Arctic Ocean started to play a role as an emission source instead of a sink, in which the POPs have constantly re-emitted and transported back to other regions in the world, mainly through LROT and volatilizing to the air, then via LRAT. The outflow of α -HCH from the Arctic is mainly through the LRAT (55% of total re-emission), whereas the majority of outflow for β -HCH mainly through the LROT (94% of total re-emission).

The monitoring concentrations of α -HCH in Arctic air and ocean indicated that volatilization from seawater exceeded absorption to seawater for this compound in 1992–1993 [34], suggesting that gas exchange became a removal pathway from a loading one since this time point (*switching point of air–ocean exchange*). Like air–ocean exchange, ocean current is also an important loading pathway, according to the description in last section. However, due to the global cutback of the HCH emissions, the removal due to the ocean current of HCHs would also be stronger than their loading through the same pathway at some point of time, which is named as the *switching point of ocean current*. α -HCH's switching point of air–water exchange happened in 1993, switching point of ocean current happened in 1985. But β -HCH's switching points happened in 1996 and 1997 for ocean current and air–water exchange, respectively. β -HCH's switching points of air–water exchange and ocean current happened obviously later than α -HCH's. These switching points of both HCHs are shown in Fig. S3.

According to a large body of evidence on monitoring data provided by numerous field studies reported in the scientific literature [43], the re-emission process is in accelerating because of the more open area of ocean water due to the melting of snowpack, sea ice, and glacier caused by global warming. The decreasing ice extent in the Arctic Ocean will effectively enhance the re-emission process. Another factor is the sea surface temperature (SST), SST is

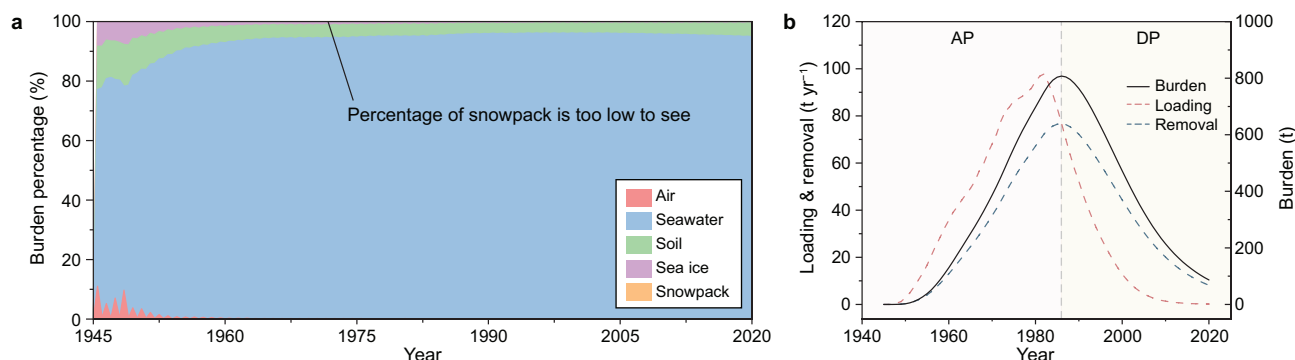


Fig. 7. a, Distribution of β -HCH's burdens in the Arctic air, water, soil, sea ice, and snowpack; b, β -HCH's burden in the Arctic Ocean.

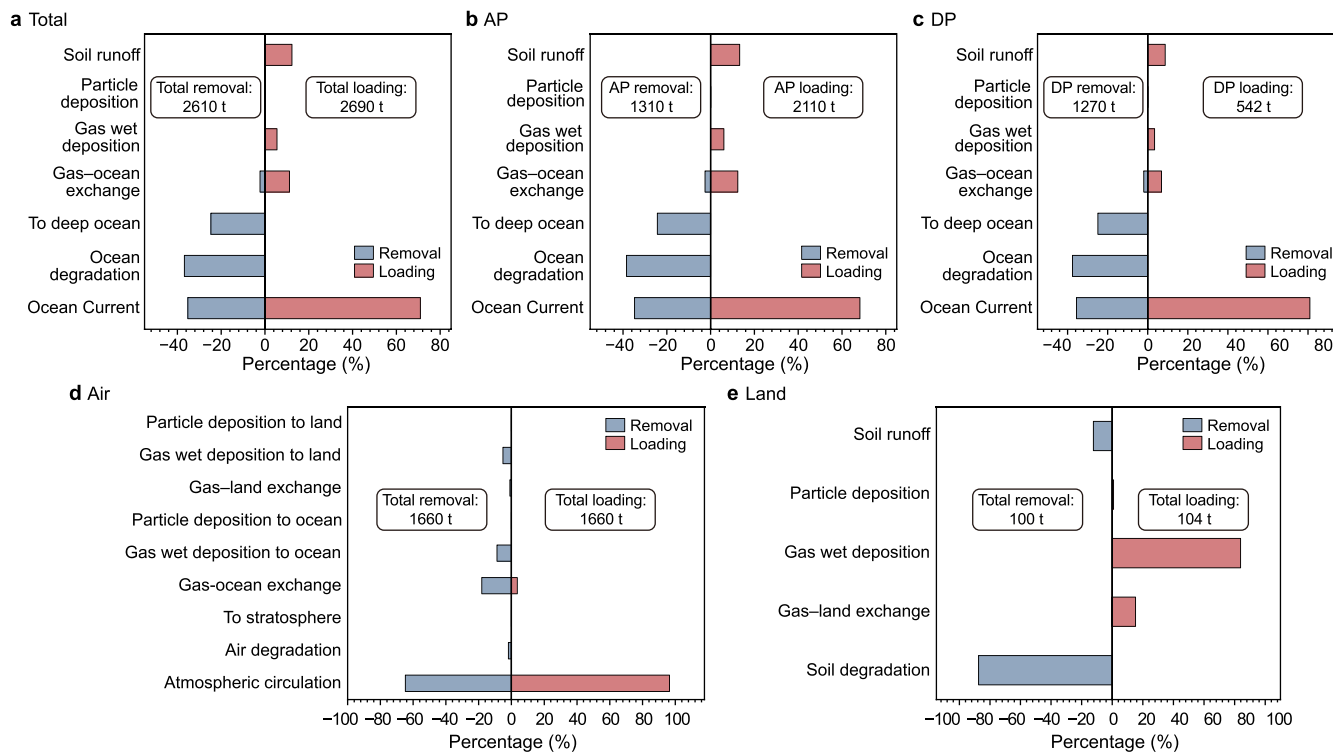


Fig. 8. a–c, Loading and removal of β -HCH in the ocean: total period (a), accumulation period (AP, b), and decay period (DP, c). d–e, Loading and removal of β -HCH in the total period in the air (d) and soil (e).

increasing by 0.03 K every year in the Arctic Ocean [44], and K_{AW} is very sensitive to temperature change. Higher temperature in the open sea water will lead to more efficient volatilization.

5.1.4. Burden

The burden of α -HCH and β -HCH after normalization is depicted in Fig. 9. The AP of α -HCH is from 1945 to 1984, and the SP is for 1984–2020, whereas the AP of β -HCH is from 1945 to 1986, and the DP is from 1986 to 2020. In the DP, the removal rate of β -HCH is obviously slower than α -HCH. The phenomenon in DP is easy to explain as β -HCH has longer half-lives in the environment. In the AP, the increase rate of α -HCH and β -HCH are similar, but the peak of β -HCH is two years later than α -HCH, which is due to the different physicochemical properties of these two isomers. Due to smaller K_{OA} than β -HCH, α -HCH is more volatile and has more percentage of the gas phase in the atmosphere available for LRAT to enter the Arctic. On the other hand, the less percentage of gaseous β -HCH in the atmosphere prefers to be sorbed in the ocean water due to its much lower K_{AW} , resulting in a major pathway of LROT for β -HCH to enter the Arctic, much slower than LRAT for α -HCH. Thus, β -HCH was firstly accumulated in Source Zone's Oceans and then transported to the Arctic Ocean through LROT. However, α -HCH was directly transported to the Arctic through LRAT and accumulated in the Arctic Ocean faster than β -HCH.

5.2. Sensitivity analysis and influence of chemical properties

As a pair of HCH isomers, the environmental behaviors of α -HCH and β -HCH are widely compared [10,16,24] as they can represent two kinds of POPs: “flyer” and “swimmer”. “Flyer” prefers long-range transport through atmospheric circulation, whereas the transport force of “swimmer” is provided by the ocean current. According to the preview study [16], this difference is believed to be

mainly caused by the air–water partition coefficient (K_{AW}). With the help of sensitivity analysis, this study further clarifies that the differences in their fates result from the comprehensive effects of their various properties.

5.2.1. Loading to the Arctic Ocean

Section 5.1.1 shows the loading difference that α -HCH mainly through LRAT's way and β -HCH mainly through LROT's way has been quantitatively compared. Fig. S4a shows the variance contribution and direction of properties to the difference.

Surprisingly, half-life in soil (HL_{Soil}) is an important parameter for α -HCH's both LRAT and LROT inflow pathways (45% and 46%, respectively). A probable reasonable explanation is that most of the HCHs deposited in the soil retained around 80% of α -HCH in the Source Zone, according to the AMBBM 2.0. The half-life of α -HCH in the soil would significantly affect its amount in the Source Zone and thus the loading to the Arctic Ocean. Another parameter, HL_{Water} , is also important for α -HCH's LROT loading to the Arctic Ocean as it directly affects its concentrations in inflow ocean currents.

In Source Zone, soil only contained 60% β -HCH, thus HL_{Soil} was not so important as that for α -HCH. HL_{Water} became the principal factor influencing β -HCH's loading through LROT. The principal

Table 2
 β -HCH vs. α -HCH loading to the Arctic Ocean.

| | | α -HCH | | β -HCH | |
|-------|--------------------|---------------|------------|--------------|------------|
| | | Flux (t) | Percentage | Flux (t) | Percentage |
| Total | | 52300 | 100% | 2690 | 100% |
| | Gas–ocean exchange | 30900 | 59% | 301 | 11% |
| | Gas wet deposition | 5390 | 10% | 147 | 5% |
| | Deposition | 11.7 | 0% | 1.54 | 0% |
| | Ocean current | 11600 | 22% | 1910 | 71% |
| | River inflow | 4420 | 8% | 331 | 12% |

factor influencing β -HCH's loading through LRAT is K_{AW} (58%), which is significantly higher than α -HCH (16%). The possible explanation is as follows. According to a calculation, the main influence of K_{AW} on air–water exchange is volatilization, but its influence on absorption is weak for α -HCH and β -HCH. Because of the very low K_{AW} value and abundant precipitation, β -HCH's deposition in the Source Zone is highly influenced by gaseous wet deposition, which is highly relative to K_{AW} value. Thus, the increase of K_{AW} can both strengthen β -HCH's total deposition and weaken its volatilization in the Source Zone. Then, β -HCH's K_{AW} -dependent air concentration in the Source Zone directly affects atmospheric Arctic inflow. But for α -HCH, whose main deposition method is absorption, the increase of K_{AW} can only weaken the volatilization and has little influence on deposition. This explanation can be supported by the modeling result from AMBBM 2.0.

Although K_{AW} can influence the loading of α -HCH and β -HCH through LRAT, it can hardly alter the loading of HCHs through LROT, especially for β -HCH. The reason is that β -HCH's burden in the ocean is far larger than in the air and the influence on the ocean caused by air–water mass transfer is limited.

This study also evaluated properties' influence on the fraction of loading through LROT, which equals LROT's loading/(LROT's loading + LRAT's loading). For α -HCH, HL_{Soil} is no longer the main influence factor, which indicates HL_{Soil} 's influence on LROT's loading and LRAT's loading are close. Instead, K_{AW} becomes the most important factor. By contrast, the main factor of β -HCH is the HL_{Water} , which dominates β -HCH concentration in the ocean and has little effect on air concentration because β -HCH has strong solubility and is hard to volatile.

5.2.2. Re-emission from the Arctic Ocean

After the switching points of gas–water exchange, the volatilization dominated the air–water exchange, and the re-emission became the mainstream, leading to the Arctic Ocean becoming a secondary emission source. After the switching points of ocean currents, the direction of the net flux due to LROT changed from loading to removal. As mentioned above, most of the α -HCH re-emits through the LRAT's way, and the LROT's way dominates the β -HCH. The variance contribution of each property is given in Fig. S4b.

HL_{Water} and HL_{Soil} are the key parameters that affect the LROT's re-emission for both chemicals because most of α -HCH and β -HCH are all contained in ocean and soil (Fig. 7a). Comparing with α -HCH, LROT's re-emission of β -HCH is more sensitive to HL_{Water} . For LRAT's re-emission, besides HL_{Water} , K_{AW} is another important factor because the increase of K_{AW} will effectively enhance volatilization

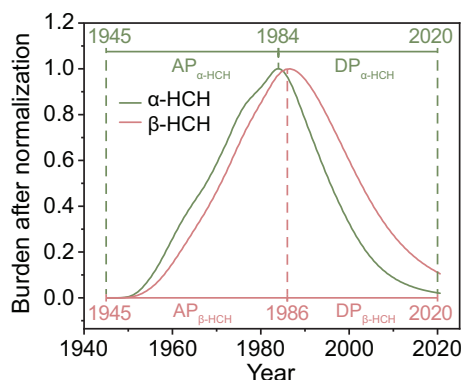


Fig. 9. Burden of α -HCH and β -HCH after normalization.

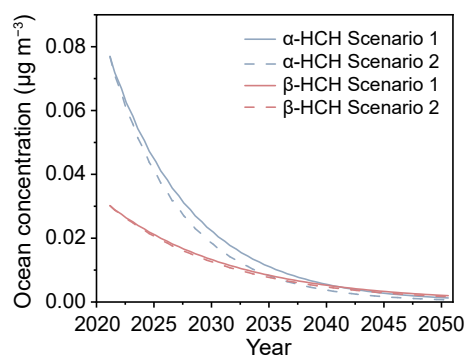


Fig. 10. Predicted concentration of β -HCH and α -HCH in the Arctic Ocean. The pink lines represent β -HCH; the blue lines represent α -HCH; the solid lines represent scenario 1, and the dashed lines represent scenario 2.

from water. Finally, the properties' influence on the fraction of LROT's re-emission is also estimated. K_{AW} is almost the only parameter determining this fraction for both isomers. A reasonable explanation is that HL_{Water} and HL_{Soil} similarly influence the re-emission through LRAT and LROT.

5.2.3. Burden in the Arctic Ocean

From the sensitivity analysis in Fig. S4c, it was found that HL_{Water} is the most important parameter determining the burden of α -HCH and β -HCH in the Arctic Ocean.

5.3. Predictions for 2020–2050 and the influence of climate

Two scenarios are assumed to predict possible concentration variation with the influence of climate change in the future. Scenario 1 assumes in 2020–2050; meteorological data will keep the same average values as in the past years; Scenario 2 is based on the climate model's results on RCP 8.5 warming assumption [45–47], where during 2020–2050, air temperature in the Arctic will increase by 2 K, ocean temperature will increase by 1 K, Sea ice area will decrease by 50%, rainfall will increase by 20%. The results are given in Fig. 10. We found that the different climate factors in the two scenarios considerably impact α -HCH and β -HCH's concentrations in the Arctic Ocean. α -HCH is more sensitive to climate change, which causes a 1.5–46% decline of its levels in the Arctic Ocean, while only a 0.3–16% decrease in the concentrations of β -HCH due to climate change.

According to the predicted results by the model, in 2021, the concentration of α -HCH in the Arctic Ocean is 2–3 times larger than β -HCH. However, because β -HCH's removal rate is slower than α -HCH, the concentration of β -HCH will finally exceed α -HCH (Scenario 1: in 2041, Scenario 2: in 2036). In 2050, there will be 4.4–5.3 t of β -HCH and 1.8–3.4 t of the α -HCH left in the Arctic Ocean.

6. Conclusion

In the present study, a Fugacity Level-IV box model (AMBBM 2.0) is developed to estimate the historical fate of β -HCH in the Arctic, which is well verified by the monitoring data. This model will advance our understanding of the environmental transport, transfer, and fate of both β -HCH and α -HCH in the Arctic. The historical burden of β -HCH was divided into two periods: accumulation period (AP) and decay period (DP). In AP, the burden in the Arctic Ocean increased, resulting from the continuous loading from the Source Zone. In DP, the Arctic Ocean's burden of β -HCH decreases sharply. This study quantitatively expounds the difference

between α -HCH and β -HCH in the loading to, removal from, and burden in the Arctic Ocean and reveals how chemicals' different physical-chemical properties cause their different fate in the Arctic Ocean. LRAT is the main pathway for α -HCH's entering and being removed from the Arctic Ocean, while β -HCH entering and leaving the Arctic mainly through the LROT, and the divergence of the pathways is due to their different physical-chemical properties. It is found that K_{AW} and the half-lives in water and soil are major parameters influencing the two chemicals' fate in the Arctic Ocean. The influence of climate change is also considered in the model to forecast β -HCH's burden in the future.

Declaration of competing interests

The authors declare that they have no known competing financial interests or personal relationships that could have appeared to influence the work reported in this paper.

Acknowledgements

This work was supported by the National Natural Science Foundation of China (No. 42077341), Natural Science Foundation of Heilongjiang Province of China (No. LH2021E096), State Key Laboratory of Urban Water Resource and Environment (Harbin Institute of Technology) (No.2022TS05), and the Polar Academy, Harbin Institute of Technology (No. PA-HIT-201901), and the support from Heilongjiang Provincial Key Laboratory of Polar Environment and Ecosystem (HPKLPPE), Harbin Institute of Technology. We would also like to acknowledge that the air monitoring dataset from Alert, Nunavut used in this study was collected with funding from Canada's Northern Contaminants Program (Crown-Indigenous Relations and Northern Affairs Canada).

Appendix A. Supplementary data

Supplementary data to this article can be found online at <https://doi.org/10.1016/j.ese.2022.100229>.

References

- [1] F.W. Kutz, P.H. Wood, D.P. Bottimore, Organochlorine pesticides and polychlorinated biphenyls in human adipose tissue, *Rev. Environ. Contam. Toxicol.* 120 (1991) 1–82.
- [2] Y.F. Li, Global gridded technical hexachlorocyclohexane usage inventories using a global cropland as a surrogate, *J. Geophys. Res. Atmos.* 104 (D19) (1999) 23785–23797.
- [3] Y.F. Li, Global technical hexachlorocyclohexane usage and its contamination consequences in the environment: from 1948 to 1997, *Sci. Total Environ.* 232 (3) (1999) 121–158.
- [4] Y.F. Li, R.W. Macdonald, Sources and pathways of selected organochlorine pesticides to the Arctic and the effect of pathway divergence on HCH trends in biota: a review, *Sci. Total Environ.* 342 (1) (2005) 87–106.
- [5] S. Tanabe, R. Tatsukawa, Chlorinated hydrocarbons in the North Pacific and Indian Oceans, *J. Oceanogr. Soc. Jpn.* 36 (4) (1980) 217–226.
- [6] G.W. Patton, M.D. Walla, T.F. Bidleman, L.A. Barrie, Polycyclic aromatic and organochlorine compounds in the atmosphere of northern Ellesmere Island, Canada, *J. Geophys. Res. Atmos.* 96 (D6) (1991) 10867–10877.
- [7] R.W. Macdonald, L.A. Barrie, T.F. Bidleman, M.L. Diamond, D.J. Gregor, R.G. Semkin, W.M.J. Strachan, Y.F. Li, F. Wania, M. Alae, L.B. Alexeeva, S.M. Backus, R. Bailey, J.M. Bowers, C. Gobeil, C.J. Halsall, T. Harner, J.T. Hoff, L.M.M. Jantunen, W.L. Lockhart, D. Mackay, D.C.G. Muir, J. Pudykiewicz, K.J. Reimer, J.N. Smith, G.A. Stern, W.H. Schroeder, R. Wagemann, M.B. Yunker, Contaminants in the Canadian Arctic: 5 years of progress in understanding sources, occurrence and pathways, *Sci. Total Environ.* 254 (2) (2000) 93–234.
- [8] R.W. Macdonald, T. Hamer, J. Fyfe, H. Loeng, T. Weingartner, AMAP Assessment 2002: the Influence of Global Change on Contaminant Pathways to, within, and from the Arctic, Arctic Monitoring and Assessment Programme, AMAP, 2003.
- [9] Y.F. Li, T.F. Bidleman, L.A. Barrie, L.L. McConnell, Global hexachlorocyclohexane use trends and their impact on the Arctic atmospheric environment, *Geophys. Res. Lett.* 25 (1) (1998) 39–41.
- [10] Y.F. Li, R.W. Macdonald, J.M. Ma, H. Hung, S. Venkatesh, Historical alpha-HCH budget in the Arctic Ocean: the Arctic mass balance box model (AMBBM), *Sci. Total Environ.* 324 (1–3) (2004) 115–139.
- [11] Y. Li, T. Bidleman, Correlation between global emissions of alpha-hexachlorocyclohexane and its concentrations in the Arctic air, *J. Environ. Info.* 1 (1) (2003) 52–57.
- [12] L.A. Barrie, D. Gregor, B. Hargrave, R. Lake, D. Muir, R. Shearer, B. Tracey, T. Bidleman, Arctic contaminants: sources, occurrence and pathways, *Sci. Total Environ.* 122 (1–2) (1992) 1–74.
- [13] Y.F. Li, M.T. Scholtz, B.J. van Heyst, Global gridded emission inventories of alpha-hexachlorocyclohexane, *J. Geophys. Res. Atmos.* 105 (D5) (2000) 6621–6632.
- [14] F. Wania, D. Mackay, Global chemical fate of α -hexachlorocyclohexane. 2. Use of a global distribution model for mass balancing, source apportionment, and trend prediction, *Environ. Toxicol. Chem.* 18 (7) (1999) 1400–1407.
- [15] K. Adare Jensen, R. Shearer, Canadian Arctic contaminants assessment report, in: Indian and Northern Affairs Canada: Ottawa vol. 460, 1997.
- [16] Y.F. Li, R.W. Macdonald, L.M.M. Jantunen, T. Harner, T.F. Bidleman, W.M.J. Strachan, The transport of beta-hexachlorocyclohexane to the western Arctic Ocean: a contrast to alpha-HCH, *Sci. Total Environ.* 291 (1–3) (2002) 229–246.
- [17] P.F. Hoekstra, T.M. O'Hara, A.T. Fisk, K. Borgá, K.R. Solomon, D.C.G. Muir, Trophic transfer of persistent organochlorine contaminants (OCs) within an Arctic marine food web from the southern Beaufort–Chukchi Seas, *Environ. Pollut.* 124 (3) (2003) 509–522.
- [18] L. Shen, F. Wania, Y.D. Lei, C. Teixeira, D.C.G. Muir, T.F. Bidleman, Hexachlorocyclohexanes in the North American atmosphere, *Environ. Sci. Technol.* 38 (4) (2004) 965–975.
- [19] J.R. Kucklick, W.D.J. Struntz, P.R. Becker, G.W. York, T.M. O'Hara, J.E. Bohonowych, Persistent organochlorine pollutants in ringed seals and polar bears collected from northern Alaska, *Sci. Total Environ.* 287 (1) (2002) 45–59.
- [20] S. Mössner, K. Ballschmiter, Marine mammals as global pollution indicators for organochlorines, *Chemosphere* 34 (5) (1997) 1285–1296.
- [21] S. Mössner, T.R. Spraker, P.R. Becker, K. Ballschmiter, Ratios of enantiomers of alpha-HCH and determination of alpha-, beta-, and gamma-HCH isomers in brain and other tissues of neonatal Northern Fur seals (*Callorhinus ursinus*), *Chemosphere* 24 (9) (1992) 1171–1180.
- [22] S. Tanabe, J.-K. Sung, D.-Y. Choi, N. Baba, M. Kiyota, K. Yoshida, R. Tatsukawa, Persistent organochlorine residues in northern Fur seal from the Pacific coast of Japan since 1971, *Environ. Pollut.* 85 (3) (1994) 305–314.
- [23] P.F. Hoekstra, T.M. O'Hara, S.J. Pallant, K.R. Solomon, D.C.G. Muir, Bioaccumulation of organochlorine contaminants in bowhead whales (*Balaena mysticetus*) from barrow, Alaska, *Arch. Environ. Contam. Toxicol.* 42 (4) (2002) 497–507.
- [24] H. Wöhrnschimmel, P. Tay, H. von Waldow, H. Hung, Y.-F. Li, M. MacLeod, K. Hungerbühler, Comparative assessment of the global fate of alpha- and beta-Hexachlorocyclohexane before and after phase-out, *Environ. Sci. Technol.* 46 (4) (2012) 2047–2054.
- [25] Y.F. Li, W.L. Ma, M. Yang, Prediction of gas/particle partitioning of polybrominated diphenyl ethers (PBDEs) in global air: a theoretical study, *Atmos. Chem. Phys.* 15 (4) (2015) 1669–1681.
- [26] R. Kwok, Arctic sea ice thickness, volume, and multiyear ice coverage: losses and coupled variability (1958–2018), *Environ. Res. Lett.* 13 (10) (2018), 105005.
- [27] M. Steele, S. Dickinson, The phenology of Arctic Ocean surface warming, *J. Geophys. Res.*: Oceans 121 (9) (2016) 6847–6861.
- [28] Y.F. Li, M.T. Scholtz, B.J. Van Heyst, Global gridded emission inventories of β -hexachlorocyclohexane, *Environ. Sci. Technol.* 37 (16) (2003) 3493–3498.
- [29] T. Harner, T.F. Bidleman, Octanol-air partition coefficient for describing particle/gas partitioning of aromatic compounds in urban air, *Environ. Sci. Technol.* 32 (10) (1998) 1494–1502.
- [30] Y.F. Li, W.L. Ma, M. Yang, Prediction of gas/particle partitioning of polybrominated diphenyl ethers (PBDEs) in global air: a theoretical study, *Atmos. Chem. Phys.* 15 (4) (2015) 1669–1681.
- [31] M. Hauck, M.A.J. Huijbregts, A. Hollander, A.J. Hendriks, D. van de Meent, Modeled and monitored variation in space and time of PCB-153 concentrations in air, sediment, soil and aquatic biota on a European scale, *Sci. Total Environ.* 408 (18) (2010) 3831–3839.
- [32] F. Wong, H. Hung, H. Dryfhout-Clark, W. Aas, P. Bohlin-Nizzetto, K. Breivik, M.N. Mastromonaco, E.B. Lundén, K. Ólafsdóttir, Á. Sigurðsson, K. Vorkamp, R. Bossi, H. Skov, H. Hakola, E. Barresi, E. Sverko, P. Fellin, H. Li, A. Vlasenko, M. Zapevalov, D. Samsonov, S. Wilson, Time trends of persistent organic pollutants (POPs) and Chemicals of Emerging Arctic Concern (CEAC) in Arctic air from 25 years of monitoring, *Sci. Total Environ.* 775 (2021), 145109.
- [33] J. Wang, R.P.J. Hoondert, N.W. Thunnissen, D. van de Meent, A.J. Hendriks, Chemical fate of persistent organic pollutants in the arctic: evaluation of simplebox, *Sci. Total Environ.* 720 (2020).
- [34] L.M. Jantunen, T.F. Bidleman, Air-water gas exchange of hexachlorocyclohexanes (HCHs) and the enantiomers of α -HCH in Arctic regions, *J. Geophys. Res.* 101 (1996) 28837–28846.
- [35] M.H. Hermanson, E. Isaksson, R. Hann, C. Teixeira, D.C.G. Muir, Atmospheric deposition of organochlorine pesticides and industrial compounds to seasonal surface snow at four glacier sites on Svalbard, 2013–2014, *Environ. Sci. Technol.* 54 (15) (2020) 9265–9273.
- [36] M. Cai, Y. Ma, Z. Xie, G. Zhong, A. Moeller, H. Yang, R. Sturm, J. He,

- R. Ebinghaus, X.-Z. Meng, Distribution and air-sea exchange of organochlorine pesticides in the North Pacific and the Arctic, *J. Geophys. Res. Atmos.* 117 (2012).
- [37] P. Casal, J. Castro-Jiménez, M. Pizarro, A. Katsoyiannis, J. Dachs, Seasonal soil/snow-air exchange of semivolatile organic pollutants at a coastal arctic site (Tromsø, 69°N), *Sci. Total Environ.* 636 (2018) 1109–1116.
- [38] Y.-F. Li, T. Harner, L. Liu, Z. Zhang, N.-Q. Ren, H. Jia, J. Ma, E. Sverko, Polychlorinated biphenyls in global air and surface soil: distributions, air-soil exchange, and fractionation effect, *Environ. Sci. Technol.* 44 (8) (2010) 2784–2790.
- [39] M. Pučko, G.A. Stern, D.G. Barber, R.W. Macdonald, K.A. Warner, C. Fuchs, Mechanisms and implications of α -HCH enrichment in melt pond water on arctic Sea Ice, *Environ. Sci. Technol.* 46 (21) (2012) 11862–11869.
- [40] K.M. Hansen, C.J. Halsall, J.H. Christensen, J. Brandt, L.M. Frohn, C. Geels, C.A. Skjøth, The role of the snowpack on the fate of α -HCH in an atmospheric chemistry-transport model, *Environ. Sci. Technol.* 42 (8) (2008) 2943–2948.
- [41] Q. Sun, C. Miao, Q. Duan, H. Ashouri, S. Sorooshian, K.-L. Hsu, A review of global precipitation data sets: data sources, estimation, and intercomparisons, *Rev. Geophys.* 56 (1) (2018) 79–107.
- [42] Q.T. Nguyen, T.B. Kristensen, A.M.K. Hansen, H. Skov, R. Bossi, A. Massling, L.L. Sørensen, M. Bilde, M. Glasius, J.K. Nøjgaard, Characterization of humic-like substances in Arctic aerosols, *J. Geophys. Res. Atmos.* 119 (8) (2014) 5011–5027.
- [43] H. Hung, C. Halsall, H. Ball, T. Bidleman, J. Dachs, A. De Silva, M. Hermanson, R. Kallenborn, D. Muir, R. Suhring, X. Wang, S. Wilson, Climate Change Influence on the Levels and Trends of Persistent Organic Pollutants (POPs) and Chemicals of Emerging Arctic Concern (CEACs) in the Arctic Physical Environment - a Review, *Environmental Science-Processes & Impacts*, 2022.
- [44] K.S. Carvalho, S. Wang, Sea surface temperature variability in the Arctic Ocean and its marginal seas in a changing climate: patterns and mechanisms, *Global Planet. Change* 193 (2020), 103265.
- [45] J.E. Overland, M. Wang, J.E. Walsh, J.C. Stroeve, Future Arctic climate changes: adaptation and mitigation time scales, *Earth's Future* 2 (2) (2014) 68–74.
- [46] R. Bintanja, The impact of Arctic warming on increased rainfall, *Sci. Rep.* 8 (1) (2018), 16001-16001.
- [47] Q. Shu, Q. Wang, M. Arthun, S. Wang, Z. Song, M. Zhang, F. Qiao, Arctic Ocean Amplification in a warming climate in CMIP6 models, *Sci. Adv.* 8 (30) (2022), eabn9755.